FEBS Letters

FEBS PRESS science publishing by scientists

# Abundance of D-2-hydroxyglutarate in G2/M is determined by FOXM1 in mutant IDH1-expressing cells

Kancharana Bala Bhaskara Rao[1,2], Kumar Katragunta[3], Uma Maheswara Sarma[3] and Nishant Jain[1,2]

1 Department of Applied Biology, CSIR-Indian Institute of Chemical Technology, Hyderabad, India
2 Academy of Scientific and Innovative Research (AcSIR), New Delhi, India
3 Organic Synthesis and Process Chemistry, CSIR-Indian Institute of Chemical Technology, Hyderabad, India

**Correspondence**
N. Jain, Department of Applied Biology, CSIR-Indian Institute of Chemical Technology, Uppal Road, Tarnaka, Hyderabad 500-007, Telangana State, India
Tel: +91-40-27191862
E-mail: nishant.iict@gov.in

(Received 26 March 2019, revised 22 May 2019, accepted 7 June 2019, available online 4 July 2019)

doi:10.1002/1873-3468.13500

Edited by Angel Nebreda

**Isocitrate dehydrogenases (IDHs) are metabolic enzymes that are mutated in several cancers, resulting in overproduction of D-2-hydroxyglutarate (D-2HG). However, the signalling pathways and factors that regulate mutant IDHs or their metabolites remain elusive. Here, we report that in synchronized cells and cells treated with anti-mitotic agents, wild-type and mutant IDH proteins are induced maximally in G2/M. Moreover, mutant IDH1-expressing cells arrested in G2/M harbour high D2HG levels. Genetic or pharmacological perturbation of Forkhead box protein M1 (FOXM1) abrogates the levels of IDH1 mRNA, protein and D2HG in G2/M. Conversely, overexpression of FOXM1 or hyperactive FOXM1 activates the IDH1 promoter and increases the abundance of its protein levels. In summary, our results show that in G2/M, higher D2HG levels are dependent on FOXM1-mediated transcription of IDH1.**

**Keywords:** cell cycle; D-2HG; FOXM1; G2/M; IDH1; IDH2

Isocitrate dehydrogenases 1 and 2 (IDH1/2) catalyse the conversion of isocitrate to α-ketoglutarate (α-KG) with the production of NAPDH. Mutations in IDH1/2, especially in its catalytic domain, are known to be associated with gliomas, acute myeloid leukaemia, chondrosarcomas and cholangiocarcinomas [1–4]. These mutations result in neomorphic activity of IDH1/2 and reduce α-KG to D-2-hydroxyglutarate (D-2HG) [5]. This leads to increased consumption of NADPH, thus mutant IDH1 cells expedite higher rates of pentose phosphate pathway to produce NAPDH [6]. Furthermore, D-2HG is structurally similar to α-KG and hence has been found to competitively inhibit α-KG utilizing enzymes. A gamut of TET-hydroxylases and Jumonji domain-containing histone demethylases are inhibited by D-2HG [7,8]. Consequently, the overproduced D-2HG effectively contributes to increased methylation on CpG islands and histones. To date, major research in the area of oncogenic IDH1 and IDH2 are focused on elucidation of the role of D-2HG in tumours [9]. Moreover, D-2HG is assumed to be constitutively produced in mutant IDH1 expressing cells, whereas the enantiomer L-2HG is selectively produced under hypoxia [10–12]. However, not much is known about the cellular regulation of neomorphic IDH proteins or their associated metabolite, D-2HG.

Continuous cultures of budding yeast grown under nutrient-limiting conditions demonstrated periodicity in the expressions of many metabolic genes. Among them, yeast mitochondrial IDH1 mRNA was also temporally induced. Taken together, the yeast metabolic

**Abbreviations**
CA4, combretastatin A4; CHR, cell cycle genes homology region; D-2HG, D-2-hydroxyglutarate; FOXM1, Forkhead box M1; IDH1, isocitrate dehydrogenase 1; IDH2, Isocitrate dehydrogenase 2; mIDHi, mutant isocitrate dehydrogenase inhibitor; Noc, nocodazole.

cycle was shown to be coordinated with the cell cycle in nutrient-limiting conditions [13]. However, mammalian cells grow in nutrient-replete conditions; thus, a periodic expression of a majority of metabolic genes may not be the norm. But in synchronized HeLa cells, protein levels of metabolic enzymes such as PFKB3, GLS-1 and PKM2 are modulated in a cell cycle-dependent manner. Protein levels of the PFKB3 peak in mid-G1 phase, GLS1 in S-phase, and PKM2 in G2/M phase [14–16]. Moreover, glycolysis and glutamine metabolism are linked to the circadian rhythm of cancer cells [17]. Thus, the expressions of some of the metabolic enzymes in tumour cells are dependent on cell cycle or circadian oscillation. As IDH1 and IDH2 are evolutionarily conserved proteins and the yeast metabolic cycle is coordinated with the cell cycle, therefore, it is possible that the expression of the IDH1 or IDH2 proteins may show periodic expressions.

To understand whether cytosolic IDH1 and mitochondrial IDH2 enzymes show any cell cycle dependencies, we analysed the reported IDH-specific transcription factors. Sterol regulatory element-binding proteins (SREBPs) are transcription factors anchored to the endoplasmic reticulum (ER) in lipid-replete conditions. In cue to lipid-deficiency, SREBP cleavage-activating protein Scap in ER, Site-1 and Site-2 proteases in Golgi orchestrate the transport and cleavage of SREBP proteins from ER to Golgi [18]. After cleavage, SREBP proteins migrate to nucleus and activate gene expressions of enzymes involved in lipid synthesis. SREBP1a and SREBP2 were shown to bind the IDH1 promoter and regulate its mRNA and protein levels in cells cultured in lipid-deficient media [19,20]. Next, Forkhead O family of transcription factors include FOXO1 and FOXO3, these evolutionarily conserved transcription factors regulate a spectrum of cellular functions [21]. Depletion of FOXO1 and FOXO3 was shown to block IDH1 expression leading to a decrease in α-KG or D-2HG levels in specific cell lines [22]. Lastly, C/EBPβ and CHOP proteins modulate IDH1 levels under ER stress [23]. Of note, under various physiological conditions analysed in these studies, IDH2 mRNA and protein levels remain unchanged. Overall, none of these reports suggested an involvement of cell cycle in the expressions of IDH1 and IDH2. Therefore, it is essential to elucidate whether expression of IDH1 or IDH2 is cell cycle-dependent and the transcription factor(s) responsible for their regulation.

Forkhead box protein M1 (FOXM1) is a master transcription factor that regulates majority of the genes involved in G2/M [24,25]. Moreover, FOXM1 levels are elevated in variety of cancers, and inhibition of FOXM1 leads to a decreased tumour burden in cell line and mouse models [26]. Genes required for the execution of G2/M phase are precisely activated by sequential binding B-MYB-MuvB and FOXM1-MuvB to their promoters harbouring a cell cycle genes homology region (CHR), [25]. In this study, we found that IDH1 and IDH2 are temporally regulated with maximal expressions in G2/M phase. Among the IDHs, depletion of mitotic transcription factor FOXM1 in mutant IDH1 expressing cells decreases the cellular abundance of D-2HG, as mRNA and protein levels of IDH1 are abrogated.

## Materials and methods

### Cell culture, transfection and inhibitors

HT1080, SW1353 are chondrosarcoma cell lines and U87 is a glioblastoma cell line purchased from ATCC (Manassas, VA, USA). HEK 293T, HeLa, A549, MDA-MB-231 and MIA PaCa-2 cell lines were also sourced from ATCC. All the cell lines were grown in DMEM (Sigma Aldrich, Saint Louis, MO, USA, D7777) with 10% FBS (Gibco, Waltham, MA, USA, 10270-106) and 1X antibiotics Pen-Strep (Sigma Aldrich, G6784) in 5% $CO_2$ and all the cell lines were routinely tested for mycoplasma contaminations. Subconfluent populations of cell lines were split and grown in dishes or six-well plates for the assays. Polyethyleneimine (PEI; Sigma Aldrich, 408727) was used as the transfection agent. The plasmids were purified by using midi-kit from Zymo™ (Zymo Research, Irvine, CA, USA, D4201) and quantified in a NanoDrop™ (Thermo Fisher Scientific, Waltham, MA, USA) before transfections. FOXM1 inhibitors: thiostrepton (T8902) and siomycin A (S6076); IDH inhibitors: mIDH1i (SML0839), mIDH2i (SML0895) were from Sigma Aldrich. Microtubule inhibitors were from Sigma Aldrich: nocodazole (Noc; 20 ng·mL$^{-1}$; M1404), combretastatin-A4 (C7744), podophyllotoxin (P4405), paclitaxel (T7402) and were used at 0.5 μM and doxorubicin (44583) was used at 10 μM, all the treatments were performed for 18 h. D-2HG (Sigma Aldrich, H8378) and L-2HG (Sigma Aldrich, 90790) were used at 100 μM concentrations for 24 h in HT1080 cells. The double-thymidine block was performed to synchronize HT1080, SW1353 and U87 cells, where 2 mM thymidine (Sigma Aldrich, T1895) was used for the first block for 17 h, then released for 9 h, and blocked again with 2 mM thymidine for 17 h [25].

### Transfections

HEK 293T cells were seeded with 0.8 million cells in 60 mm dish and next day cells were transfected with respective plasmids as mentioned in figure legends. In all the

transfections, salmon sperm DNA was used to make up the total DNA concentration to 2 μg. Transfections were performed for 4 h with 6 μg of polyethylenimine (PEI) in serum-free media and cells were allowed to grow for another 20 h [27]. Incorporation of salmon sperm DNA with plasmids improves the efficiency of transfection, as empty plasmids do not compete for the endogenous proteins [28]. The protein lysates were dissolved in 1X SDS sample buffer of 150 μL volume. The proteins were resolved by SDS/PAGE and the protein levels were determined using appropriate antibodies [29].

## Expression constructs

Total RNA was isolated from three 10 cm dishes of HEK 293T with (Trizol™, St. Louis, MO, USA) and 500 μg of total RNA was subjected to mRNA isolation using the polystyrene oligo-dT beads. One microgram of mRNA was reverse transcribed (Superscript II; Invitrogen, Waltham, MA, USA) and used as a template for PCRs [30]. Appropriate primers were used to amplify IDH1 and IDH2 genes, the PCR product was thymidine and adenine-cloned in pCR2.1-TOPO and sequenced. IDH1 and IDH2 were sub-cloned into the hemagglutinin (HA)-tagged vector. To generate mutants of HA-tagged IDH1 (R132C and H) or HA-IDH2 (R140Q and R172K), site-directed mutagenesis (SDM) was performed and the PCR conditions and subsequent DpnI digestions were conducted as described [31]. T7-FOXM1 was a generous gift from P. Raychaudhuri (University of Illinois, Chicago, IL, USA) and HA-Lin 54 was from S. Gaubatz (Biozentrum, University of Wuerzburg, Germany). T7-ΔN-FOXM1 (N-terminal deleted T7 tag FOXM1 expression construct) was PCR amplified using T7-FOXM1 as a template and cloned into an untagged pcDNA and Add Track-CMV expression vector. Flag-FOXM1 PCR amplified using T7-FOXM1 as a template and was cloned into EcoRI/ XbaI sites of pCMV-3XFLAG vector (Sigma Aldrich, E7283).

## Western blot

Cells were washed three times 1X PBS and harvested in 1X sample buffer. Equal amounts of proteins were subjected and separated on a 10% SDS/PAGE and transferred onto a nitrocellulose membrane using semi-dry transfer apparatus. The blots were washed three times with 1X Tris-buffered-saline with 1% tween 20 (TBST) containing 0.1% Tween-20 and blocked for 1 h at room temperature using 5% non-fat dry milk. Later, the blots were incubated with appropriate dilutions of the antibodies either 1 : 500 or 1 : 1000 in TBST with 10% of blocking solution. After 2 h of incubation, the blots were washed thrice with 1X TBST and incubated with anti-rabbit or anti-mouse HRP conjugated antibody for 1 h and washed again, then subjected to enhanced chemiluminescence (ECL) detection [29]. The primary antibodies used in the study are listed in Table 1. Anti-Rabbit IgG (whole molecule)–peroxidase (A6154; Sigma Aldrich) was used at 1 : 5000 to detect IDH1, IDH2, IDH3A, CyclinB1 and GFP. Anti-Mouse IgG (whole molecule)–peroxidase (A9044; Sigma Aldrich) was used at 1 : 5000 to detect Cyclin A, α-tubulin, histone3 $Ser^{10}$ phosphorylation (pH3Ser10), T7-tag and donkey anti-goat IgG- peroxidase (sc-2020; Santa Cruz, Dallas, TX, USA) was used at 1 : 5000 to detect firefly luciferase protein. Freshly prepared ECL buffer of 100 mM Tris/HCl pH 8.8, 1.25 mM luminol, 2 mM 4IBPA and 5.3 mM hydrogen peroxide was used for every ECL detection [32]. Kodak X-ray films were used to develop the immunoblots.

## IDH1 promoter

Genomic DNA from three 100 mm dishes of HEK 293T was isolated using the Qiagen-DNA (Hilden, Germany) prep kit and after quantification, 100 ng of genomic DNA was used as a template for PCR to amplify IDH1 promoter with primers was as described [20]. After PCR, the product was TA-cloned, sequenced and sub-cloned into a pGL4-basic vector. Appropriate primers were used to generate two deletion constructs of IDH1 promoter 532 and 219 bp using a common reverse primer that encompasses transcription start site. Zymo™ purified plasmids were used for transfections in six-well plates of HEK 293T, where 200 ng of promoter vector was co-transfected with FOXM1 or ΔN-FOXM1 for 30 h [33]. Finally, cells were harvested in 1X sample buffer and subjected to SDS/PAGE and immunoblot analysis.

## FOXM1 knockout by CRISPR/Cas9

sgRNA targeting FOXM1 and GFP were selected from the Gecko library[34]. FOXM1, sg1: (5′-caccgCATGCCCAAC ACGCAAGTAGc-3′); and FOXM1, sg2: (5′-caccgAACT CATCTTTCGAAGCCACc-3′); and GFP, sg3: (5′-caccg GGCCACAAGTTCAGCGTGTCc-3′). Two microgram of sgRNA oligonucleotide pairs were annealed in 10 mM Tris pH 8.0 and 50 mM NaCl at 65 °C for 5 min, 37 °C for 10 min and 4 °C for 1 min. Annealed product was diluted to 1 : 20 times and ligated into 50 ng of the *BsmB*I-linearized plentiCRISPR v2 vector (Addgene; #52961, Watertown, MA, USA). Recombinant clones were identified by PCR using the gRNA primer as forward and reverse primer in the vector backbone. After sequencing, Zymo™ purified plasmids of 200 ng Lenti CRISPR v2 expressing FOXM1 sgRNAs were co-transfected with 100 ng of pMD2.G (Addgene; # 12259) and 200 ng of psPAX2 (Addgene; #12260) in HEK 293T to generate lentiviruses [35]. Total DNA content was made up to 5 μg using salmon sperm DNA and mixed with 15 μg of PEI and transfected into 10 cm dish of containing 2.5 million HEK 293T cells for 4 h [27]. Furthermore, we employed lower concentrations of the lentiviral vectors and salmon sperm

**Table 1.** Antibodies used for the study. Company locations: Millipore, Saint Louis, Missouri, USA and Promega, Madison, WI, USA.

| Primary antibody | Source | Dilution in 1X TBST with 0.5% nonfat milk or 1X PBS with 0.3% BSA | Antigen function |
|---|---|---|---|
| IDH1(41–55) (rabbit-anti-human) | Sigma AldrichSAB1100101 | 1 : 1000 | Cytosolic IDH1 oxidatively decarboxylates isocitrate to α-KG |
| IDH1(336–350) (rabbit-anti-human) | Sigma AldrichSAB1100102 | 1 : 1000 | |
| IDH2 (rabbit-anti-human) | Sigma AldrichSAB1100103 | 1 : 1000 | Mitochondrial IDH2 converts isocitrate to α-KG |
| IDH3A (rabbit-anti-human) | Sigma AldrichSAB1100033 | 1 : 1500 | IDH3A catalyses the oxidative decarboxylation of isocitrate to α-KG as part of Krebs cycle |
| CyclinB1 (rabbit-anti-human) | Sigma AldrichSAB4503501, SAB4503502 | 1 : 500 | Cyclin B1 a key regulatory protein involved in cell division. |
| α-tubulin (mouse-anti-human) | Sigma AldrichT6074 | 1 : 3000 | Microtubules are polymers composed of α-and β-tubulin which provide cellular framework |
| Cyclin A (mouse-anti-human) | Sigma AldrichC4710 | 1 : 1000 | Cyclin A binds to CDK2 kinase and promotes the G1/S and G2/M transitions |
| pH3Ser10 (mouse-anti-human) | Sigma AldrichH6409 | 1 : 1000 | Site-specific phosphorylation of core histone H3 at serine 10 occurs during cell division |
| FLAG-Peroxidase | MilliporeA8592 | 1 : 2000 | Detects FLAG-epitope tagged proteins |
| HA-Peroxidase | Sigma AldrichH6533 | 1 : 2000 | Detects HA-epitope tagged proteins |
| T7-Tag | Sigma AldrichT8823 | 1 : 2000 | Detects T7-tagged proteins |
| GFP | SigmaAldrich SAB4301138 | 1 : 2000 | Green fluorescent protein used to normalize transfection in promoter assays and adenoviral based infections |
| Firefly Luciferase | PromegaG7451 | 1 : 500 | Firefly luciferase is an enzyme which oxidizes luciferin to produce light |

DNA for optimal virus production as described [28]. After 60 h of transfection, medium was spun at 70 000 ***g*** for 2 h at 4 °C in tubes and the viral-pellet was re-suspended in 300 μL of 1% BSA containing DMEM overnight at 4 °C. On next day, 0.2 million HT1080 cells plated in six-well plates were infected with different volumes of viruses with 8 $\mu g \cdot mL^{-1}$ of polybrene for 17 h. Two days later the cells were supplemented with 1 $\mu g \cdot mL^{-1}$ puromycin for 72 h and the puromycin resistant clones were expanded and used for experiments [34].

## Cloning of shRNAs

shRNAs targeting FOXM1 were cloned into MU6pro vector under U6 promoter in BbsI and XhoI site as described [29,36,37]. The sequence of the shRNA of FOXM1 sh1; (5′-tttgGGACCACTTTCCCTACTTTttcaagagaAAAGTAGGGAAAGTGGTCCttttt-3′) and FOXM1sh2; (5′-tttgCAACAGGAGTCTAATCAAGttcaagagaCTTGATTAGACTCCTGTTGttttt-3′). FOXO1/3, SREBP1 and SREBP2 were cloned into pLKO.1 puro (Addgene; #8453), the sequences cloned were FOXO1/3 sh3, (5′-ccggGTGCCCTACTTCAAGGATAAGctcgagCTTATCCTTGAAGTAGGGCACttttg-3′); SREBP1 sh4, (5′-ccggCCAGAAACTCAAGCAGGAGAActcgagTTCTCCTGCTTGAGTTTCTGGttttg3′); SREBP2 sh5, (5′-ccggGCTGAATAAATCTGCTGTCTTctcgagAAGACAGCAGATTTATTCAGCtttttg-3′); Finally, a scrambled shRNA was used as control [22].

## Adenoviruses expressing FOXM1 shRNAs and proteins

U6 promoter-FOXM1 shRNA cassette or U6 promoter-shRNA scrambled cassettes were excised from a MU6pro vector and subcloned into HindIII/XbaI of pAdTrack vector. After recombination in AdEasier-1 cells, 500 ng of PacI digested clones were transfected into HEK 293T using PEI. Ten to twelve days post-transfection, the viruses were harvested, titred and re-amplified for another two rounds in 10 cm dishes of HEK 293T and later viruses were infected in destination cell lines according to their Multiplicity of infection [38,39]. Adenoviral FOXM1 Adsh1 targets the N-terminal of FOXM1, hence reduces the full-length FOXM1 protein and not ΔN-FOXM1. To generate adenoviral FOXM1 and Δ-FOXM1, T7-sequence was incorporated in the forward primers used to amplify FOXM1/ΔN-FOXM1 and subcloned into the pAdTrack CMV vector. Empty pAdTrack CMV vector was subjected to recombination and was used as a control. The viruses were generated similar to adenoviral FOXM1 shRNAs [38,39].

## Estimation of D-2HG levels by LC-MS/MS

Sub-confluent HT1080 in 60 mm dishes were treated with various inhibitors or infected with adenoviral FOXM1 shRNAs. Later, the cells were washed with 1X ice-cold

PBS, harvested in 3.6 mL of (80 : 20) methanol : water and centrifuged at 14 000 ***g*** for 20 min. The supernatant was taken into a fresh tube and dried in a speed-vac at 900 ***g*** at room temperature for 90 min and the dried sample was reconstituted with 100 µL of liquid chromatography–mass spectrometry (LCMS) buffer. Chromatographic separation was performed using a reverse phase XBridge™ amide column (150 × 4.6mm, 3.5 µm; Waters Corporation, Dublin, Ireland) at ambient temperature (25 °C) throughout the experiment. Mobile phase was of a 95% mixture of 20 mM ammonium acetate and 20 mM ammonium hydroxide (25% w/v) adjusted to pH of 9% and 5% acetonitrile (A), acetonitrile (B) at a flow rate of 1.0 mL·min$^{-1}$ in isocratic mode with an injection volume of 10 µL. The chromatographic analysis was performed on a Shimadzu nexera X2 UPLC system (Shimadzu Corporation, Kyoto, Japan) equipped with a quaternary pump, an online degasser (DGU-20A 5R), a thermostated auto sampler (SIL-30AC), a thermostatically controlled column compartment (CTO-20AC), and a diode array detector (PDA; SPD-M20A), which were communicated through bus module (CBM-20A). For LC-ESI-MS/MS experiments, Shimadzu triple quadrupole mass spectrometer (LCMS-8040; Shimadzu Corporation) equipped with an electrospray ionization (ESI) source was connected to the LC instrument. The ESI source parameters were set as follows: ion spray voltage, 2.5 kV; Desolvation line temperature, 300 °C; heat block temperature, 400 °C; nebulizing ($N_2$) and dry gas ($N_2$) flow rates, 3.0 and 10.0 L·min$^{-1}$, respectively. Argon gas was used as CID gas for MRM experiments. The mass analyser was operated in negative ion mode for MRM experiments with the transition of $m/z$ 147.0 → 129.0 at a collision energy if 14 eV and dwell time of 100 msec. Accurate masses were calibrated according to the manufacturer's guidelines using TQ Standard Sample (PEG, PPG and Raffinose; Shimadzu Corporation). Data were recorded and processed using the LCMS LAB SOLUTIONS v5.60 SP2 software (Shimadzu Corporation). The signal intensities obtained were normalized to cell counts from corresponding duplicate plates of HT1080 cells treated or transfected under same conditions. The fold-change represents the D-2HG levels obtained in each sample after normalization [5,40].

### Biotinylated DNA affinity purification

HEK 293T cells were co-transfected with 500 ng of Flag-FOXM1 and HA-Lin54 plasmids. After 4 h of transfection, serum free media was exchanged with complete DMEM media, and treated with Noc or siomycin or infected with adenoviral FOXM1shRNA for 20 h. Later, nuclear extracts of HEK 293T cells incubated with wild-type and mutant CHR site IDH1 promoter (962 bp) tagged with biotin; the sequence of the primers used IDH1-Prom-Biotin; 5′-TCC ACCGTTTTCTAAGGCTTCACATC-3′ (forward) and 5′-GATGATATGCTGGCGAAGAGTTGGG-3′ (reverse). The biotinylated DNA affinity purifications were performed as described [41,42]. Biotinylated pull down samples were subjected to SDS/PAGE and immunoblot analysis for Flag-FOXM1 and HA-Lin-54.

### Quantitative RT-PCR analysis

HT1080 cells plated in 60 mm dishes were treated with various anti-mitotic agents or infected with FOXM1 shRNAs was subjected to total RNA isolation using Tri-reagent. The RNA purified was run on 1% agarose gels to check its integrity followed by estimation in a Nano-drop. Two micrograms of RNA was reverse transcribed using superscript-III (Invitrogen) and dissolved in 20 µL of DEPC-treated water. A reaction mixture containing 50 ng of template and 10 ng of forward and reverse primers with 2X-sybr green was subjected to quantitative PCRs. The PCR conditions IDH1, IDH2, CyclinB1 and GAPDH were one cycle of 3 min at 95 °C, 40 cycles of 1 min at 95 °C, 30 s for 56.5 °C and 30 s for 72 °C cycles. The sequence of the primers employed for the amplification as follows: IDH1, 5′-AGAAGCATAATGTTGGCGTCA-3′ (forward) and 5′-CGTATGGTGCCATTTGGTGATT-3′ (reverse); IDH2, 5′-CGCCACTATGCCGACAAAAG-3′ (forward) and 5′-ACTGCCAGATAATACGGGTCA-3′ (reverse); CyclinB1, 5′ CGGAGAGCATCTAAGATTGGAGAGG-3′ (forward) and 5′-GCTCCTGCTGCAATTTGAGAAGG-3′ (reverse); GAPDH, 5′- TGTGGGCATCAATGGATTT GG-3′ (forward) and 5′-ACACCATGTATTCCGGGT CAAT-3′ (reverse). Fold changes in gene expressions was normalized to GAPDH mRNA [43].

### Statistical analysis

Student's $t$ test was used to calculate statistical differences. Using a two-tailed $t$ test, $P$ values for pair wise comparisons were deduced, $P < 0.05$ was considered significant.

## Results

### Protein levels of IDH1 and IDH2 peak in G2/M

We explored whether mammalian IDH1 and IDH2 proteins are expressed in tune with the cell cycle. To understand this, we opt for U87$^{WTIDH1/2}$, HT1080$^{WT/MTIDH1\text{-}R132C}$ and SW1353$^{WT/MTIDH2\text{-}R172S}$ cell lines [44,45]. These cell lines were synchronized with a double-thymidine block and released into medium without thymidine. IDH1 and IDH2 protein levels were induced by 6 h, plateaued by 9 h, decreased by 12 h of treatments in all the cell lines. Further, a precipitous drop in IDH2 and a decrease in IDH1 protein levels were found by 15 h. The changes in IDH1/2 protein levels mirrored the temporal expression pattern

of Cyclin B1, a G2/M marker, but not the S-phase marker cyclin A. To substantiate our observations, we also probed the lysates for pH3Ser10, a mitotic marker [46]. Akin to Cyclin B1, the increased protein levels of pH3Ser10 coincided with IDH1, IDH2 and Cyclin B1 temporal windows. Further, we checked the protein levels of IDH3A, a mitochondrial homolog of IDH1 and IDH2 proteins that resides in mitochondria and functions in the tricarboxylic acid cycle [47]. However, protein levels of IDH3A remain unaltered in all the cell lines tested (Fig. 1A–C). As IDH1 is frequently mutated in gliomas, we therefore, confirmed the cell cycle dependent expression of IDH1 using an antibody which detects a different epitope of IDH1. IDH1 protein levels exhibited similar temporal window, wherein protein levels peaked in G2/M (Fig. S1). In addition, IDH1 and IDH2 antibodies used in the study can detect both wild-type and mutant IDH proteins (Fig. 1D). Collectively, our results suggest that IDH1 and IDH2 proteins are activated in a cell cycle-dependent manner, with maximal induction in the G2/M phase of cell cycle.

## Anti-mitotic agents increased abundance of IDH1 and IDH2 gene and protein levels

To further corroborate our findings that IDH1 and IDH2 proteins are indeed induced in G2/M, we used a set of anti-tubulin agents such as Noc, combretastatin A4 (CA4), podophyllotoxin and paclitaxel [48]. Among the anti-mitotic agents, Noc is a tubulin depolymerisation inhibitor and is routinely used to arrest cells in prometaphase. U87, HT1080 and SW1353 cells lines were treated with the inhibitors for 18 h. Noc robustly increased IDH1 and IDH2 protein levels in all the cell lines compared to untreated or DMSO-controls. Similar to Noc, IDH1 and IDH2 protein levels were also strongly induced by the other three anti-mitotic agents. Protein levels of Cyclin B1 and pH3Ser10 were markedly increased by the pharmacological modulators of tubulin assembly. To ensure that an increase in IDH1 and IDH2 was not due to apoptosis, we also treated the cells with doxorubicin. However, protein levels of IDH1 and IDH2 remained unchanged in doxorubicin-treated cells (Fig. 2A–C). To determine, whether the enhanced IDH protein levels induced by anti-mitotic agents in G2/M were due to transcriptional activation of IDH genes, we performed RT-PCR analysis. The mRNA levels of IDH1, IDH2 and Cyclin-B1 increased in HT1080 cells treated with anti-mitotic blockers as compared to controls (Fig. 2D). Taken together, cells stalled at G2/M phase by anti-mitotic agents contain higher amounts of IDH1 and IDH2 mRNA and proteins.

## Knockdown of FOXM1 blocks IDH1 protein levels in G2/M

Isocitrate dehydrogenase 1 is frequently mutated in various primary and secondary gliomas and chondrosarcomas [49]. Therefore, we employed U87 and HT1080 cell lines as they are derived from glioma and chondrosarcomas patients. Here, we show that IDH1 is maximally activated in G2/M in these cell lines (Figs 1 and 2). Hence, we examined whether the known transcriptional activators of IDH1 played any role in this induction. We also analysed if FOXM1, a mitotic transcription factor regulates the protein levels of IDH1, as it governs the expression of more than 50 genes in G2/M [24,25]. To determine this, shRNAs of FOXO1/3, SREBP1a, SREBP2 and FOXM1 were transiently introduced into HEK 293T cells followed by Noc treatments [19,20,22]. Depletion of FOXM1 eliminated Noc-induced IDH1 levels, whereas IDH2 descend to basal levels. To substantiate our observations, protein levels of CyclinB1, a transcriptional target of FOXM1 were diminished by shFOXM1 (Fig. 3A), [50]. Next, we assessed whether depletion of FOXM1 in synchronized cell population affects IDH1 protein levels. We generated recombinant adenoviruses expressing either a scrambled or two FOXM1 specific shRNAs (Adsh1 and Adsh2) to overcome limitations of transfection. These shRNA-expressing viruses tested for their efficacy in HeLa cells strongly depleted FOXM1 protein (Fig. 3B). Next, U87 and HT1080 cells were infected with these viruses for 2 h, synchronized by double-thymidine block, IDH1 and IDH2 protein levels were analysed at 6, 9 and 12 h post-release, as these time-points manifest higher levels of IDH proteins (Fig. 1A–C). As expected, IDH1 and IDH2 protein levels were induced by 6 h post-release in uninfected or control shRNA infected cells. In contrast, cells infected with FOXM1 shRNAs, a marked depletion of IDH1 and Cyclin B1 protein levels were observed, whereas IDH2 levels moderately decreased (Fig. 3C–D). Since Noc-arrested cells harbour higher amounts of IDH1 protein (Fig. 2A–C), we checked whether knock-down of FOXM1 affects IDH1 protein levels. We observed that, a strong decrease in FOXM1 protein leads to a drop in the abundance of IDH1 and CyclinB1 proteins (Fig. 3E–F). In addition, FOXM1 shRNA infected cells showed negligible amounts of IDH1 and CyclinB1 mRNA levels (Fig. 3G). In comparison to IDH1 or CyclinB1, IDH2 mRNA or protein levels only decrease in FOXM1 shRNA infected cells, Collectively, FOXM1 deficiency results in the loss of IDH1 transcript and protein levels in G2/M.

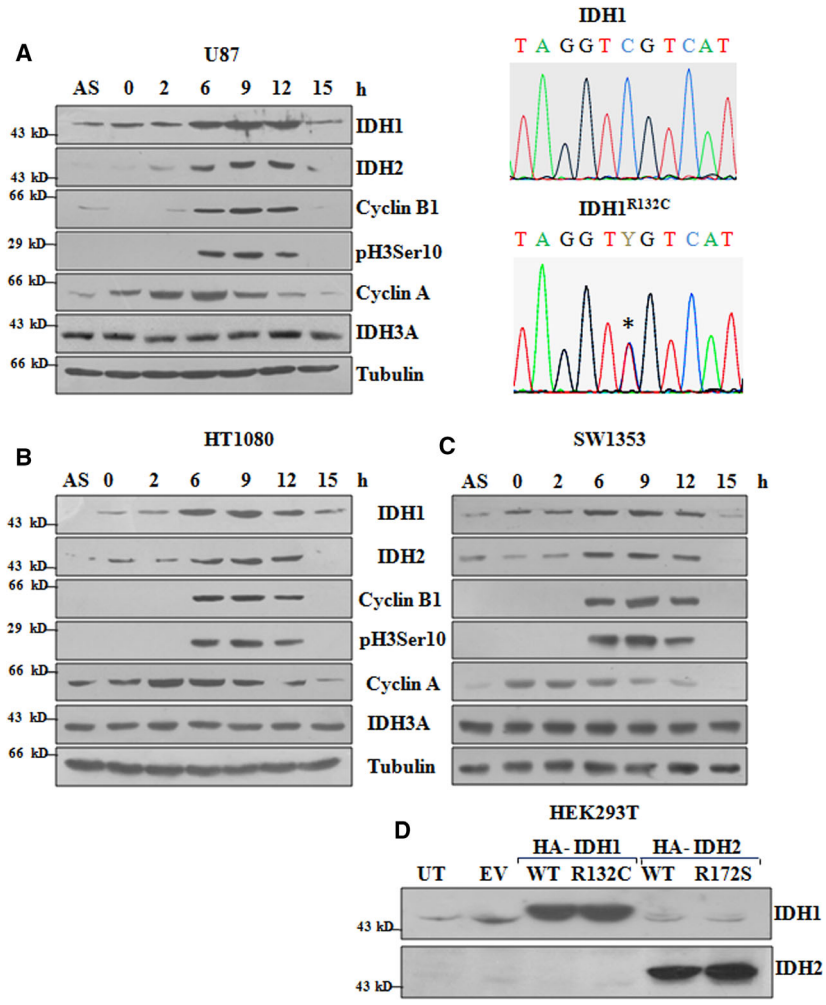


**Fig. 1.** IDH1 and IDH2 protein levels are maximum in G2/M. (A–C) U87$^{WTIDH1/2}$, HT1080$^{WT/MTIDH1\text{-}R132C}$ and SW1353$^{WT/MTIDH2\text{-}R172S}$ cell lines were synchronized using double-thymidine block. AS, represents asynchronous cell population. Whole cell lysates (WCL) were resolved by using SDS/PAGE and subjected to immunoblot analysis for IDH1, IDH2 and IDH3A. Protein levels of CyclinB1 and pH3Ser10 were used to indicate G2/M. Cyclin A was employed for S-phase marker and tubulin as a loading control. Mutation status of IDH1 was determined by genomic DNA sequencing. Blots are representative of three independent experiment ($n$ = 3). (D) HEK 293T cells were transfected with 500 ng of HA-tagged plasmids of WT or R132C-IDH1 and WT or R172S-IDH2 using PEI for 24 h. WCL were resolved by SDS/PAGE and probed with IDH1 and IDH2 antibodies.

## Pharmacological and genetic perturbation of FOXM1 abolishes IDH1 protein levels

Small molecule inhibitors are the vanguards of cancer therapy, as knock-down of FOXM1 abrogated IDH1 protein levels; we checked whether pharmacological inhibition of FOXM1 affects IDH1. To determine this, we opted for HT1080 cell line as they express mutant IDH1. Here, cells were treated with FOXM1 inhibitors siomycin A or thiostrepton (FOXM1i) or infected with FOXM1 shRNAs and co-treated with Noc to arrest in G2/M [37,51]. To rule out that, IDH1 protein is not a target of FOXM1i; mutant IDH1/2 inhibitors (mIDHi) were also co-treated with Noc [52,53]. FOXM1i and its shRNAs block FOXM1, IDH1 and Cyclin B1 protein levels, whereas IDH2 protein levels were decreased. Unlike FOXM1i, mIDHi did not alter the protein levels of IDH1 or IDH2; conforming pharmacological inhibition of FOXM1 ablates IDH1 protein levels (Fig. 4A). Further, shRNA-mediated depletion of FOXM1 aborted Noc-induced IDH1 protein levels in a panel of cell lines (Fig. S2). To confirm our findings, we performed a CRISPR/Cas9 mediated knock-out of FOXM1 in HT1080 cells. Elimination of FOXM1 protein by two FOXM1 specific-sgRNAs abrogated baseline and Noc-induced IDH1 levels (Fig. 4B). Finally, these results suggest that FOXM1 determines IDH1 protein levels.

## Ectopic FOXM1 increases IDH1

To further substantiate that FOXM1 regulates IDH1 we examined IDH1 proteins levels in HT1080 cells overexpressing FOXM1. We generated recombinant adenoviruses expressing proteins of T7-tagged full-length or an N-terminal domain deleted hyperactive FOXM1 [33]. HT1080 cells infected with FOXM1 or ΔN-FOXM1 robustly induce IDH1 and CyclinB1 proteins, in comparison, IDH2 levels moderately increase.

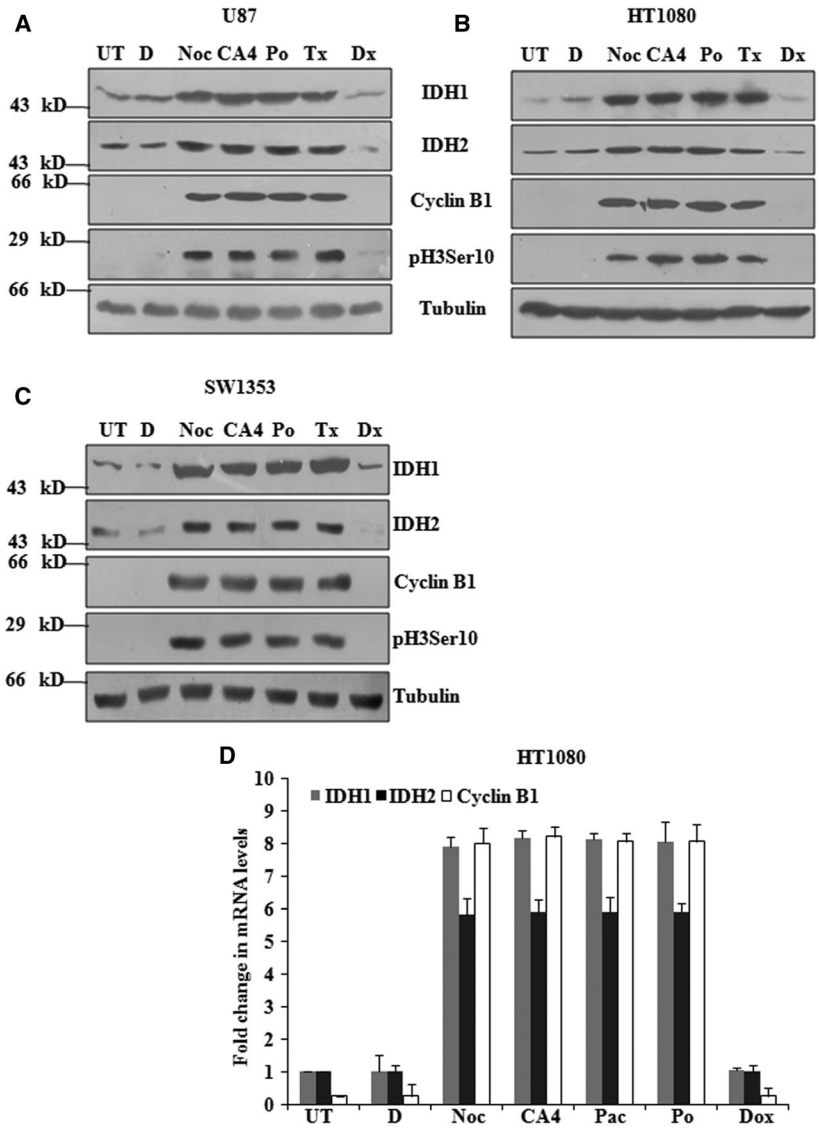


**Fig. 2.** G2/M arrested cells possess high levels of IDH1 and IDH2 proteins. (A–C) U87, HT1080 and SW1353 cells were treated with microtubule inhibitors or doxorubicin. UT, represents untreated cells and D for DMSO-treated cells. Noc (20 ng·mL$^{-1}$), CA4, Podophyllotoxin (Po) and Paclitaxel (Tx) was used at 500 nM, Doxorubicin (Dx) at 5 μM concentrations for 18 h. WCL were subjected to SDS/PAGE and immunoblot analysis for IDH1, IDH2, Cyclin B1 and pH3Ser10 using appropriate antibodies. Blots are representative of three independent experiments. (D) Quantitative RT-PCR analysis of the mRNA levels of IDH1, IDH2 and CyclinB1. GAPDH was used for normalization.

To substantiate that FOXM1 indeed activates IDH1, we performed a rescue with ΔN-FOXM1. Here, the N-terminal targeted FOXM1 shRNA (Adsh1) reduces only full-length FOXM1 protein, leaving ΔN-FOXM1 intact. Co-infection with ΔN-FOXM1 markedly rescued IDH1 protein levels in Adsh1 infected cells (Fig. 5A). Next, we investigated whether Noc-induced IDH1 protein levels are enhanced by FOXM1 or

**Fig. 3.** Down-regulation of FOXM1 blocks IDH1 and IDH2 protein in G2/M. (A) HEK 293T cells were transiently transfected with 500 ng of shRNA against FOXM1, FOXO1/3, SREBP1a or SREBP2 and 200 ng of GFP. SCR represents scrambled shRNA. After separation on SDS/PAGE, blots were probed for IDH1, IDH2 and Cyclin B1 proteins. Here, GFP was used as transfection control and tubulin as loading control. Blots are representative of two independent experiments in duplicates ($n$ = 4). (B) Hela cells were infected with control or adenoviral FOXM1 shRNAs (Adsh1 or Adsh2) for 24 h. GFP was used as an infection control and tubulin as loading control. (C–D) U87 or HT1080 cells were plated in 60 mm dishes and infected with control or Adsh1 or Adsh2 for 2 h or left uninfected. Subsequently the cells were synchronized with double-thymidine blocks. After release from thymidine, WCL were harvested at 6, 9, 12 h and western blotting was conducted for IDH1, IDH2, Cyclin B1 and FOXM1. Viruses co-express GFP from a separate promoter, so GFP served as infection control. Results represented from three independent experiments. (E, F) Adenoviral FOXM1 shRNAs were infected for 2 h in U87 or HT1080 cell lines and later treated with Noc; IDH1 and IDH2 levels were determined by immunoblotting. Blots shown are from two independent experiments performed in duplicates ($n$ = 4). (G) mRNA levels of IDH1, IDH2 and CyclinB1 levels were quantified in HT1080 cells depleted of FOXM1 and treated with or without Noc.

ΔN-FOXM1. FOXM1 and its variant increased the abundance of IDH1 compared to IDH2 (Fig. 5B). Similarly, overexpression of ΔN-FOXM1 strongly increased IDH1 in a panel of cell lines (Fig. S3). Since, knock-down and overexpression of FOXM1 modulates IDH1 expressions, we analysed whether FOXM1 activates IDH1 promoter. To determine this, we cloned the previously characterized IDH1 promoter of 962 bp

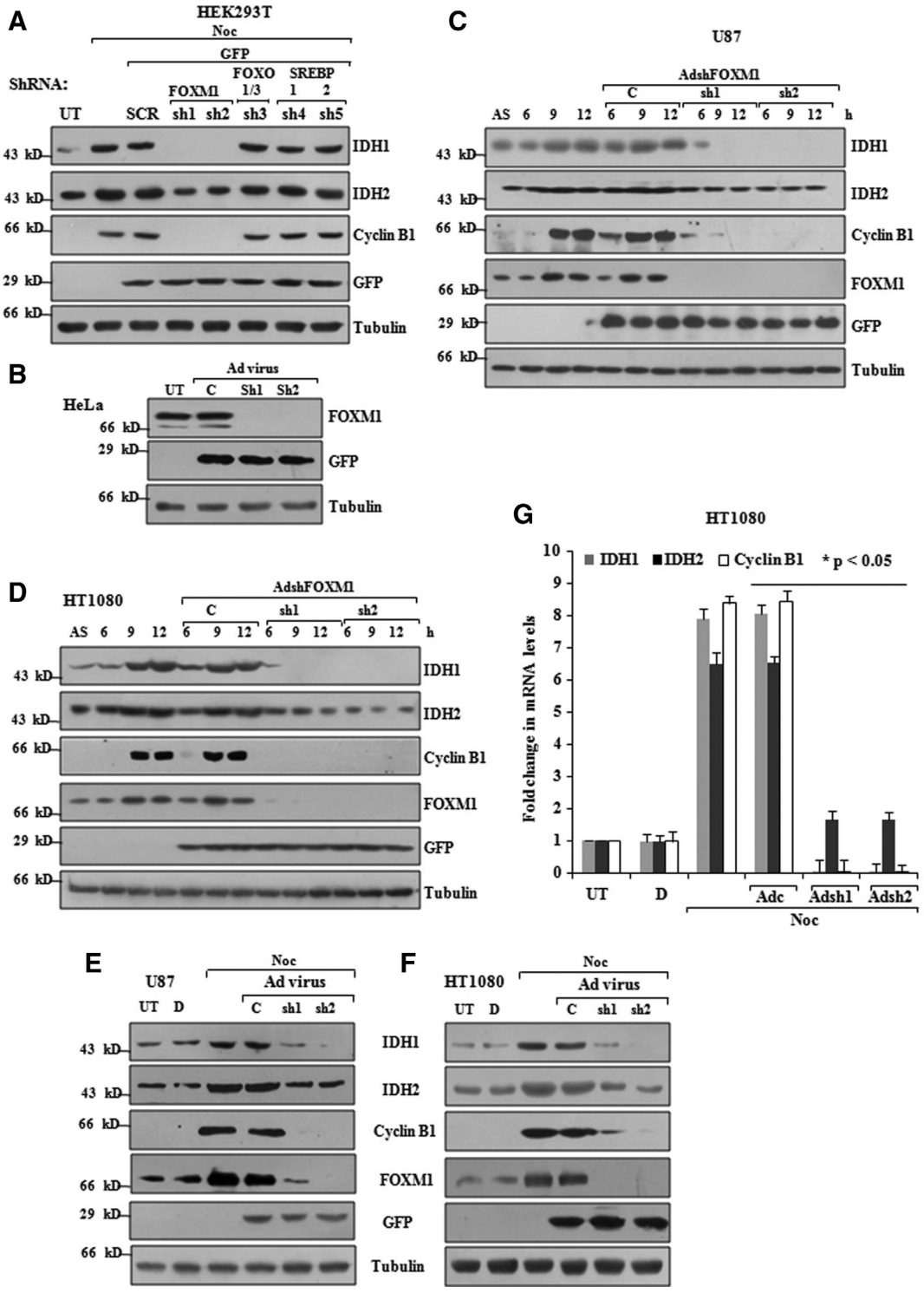

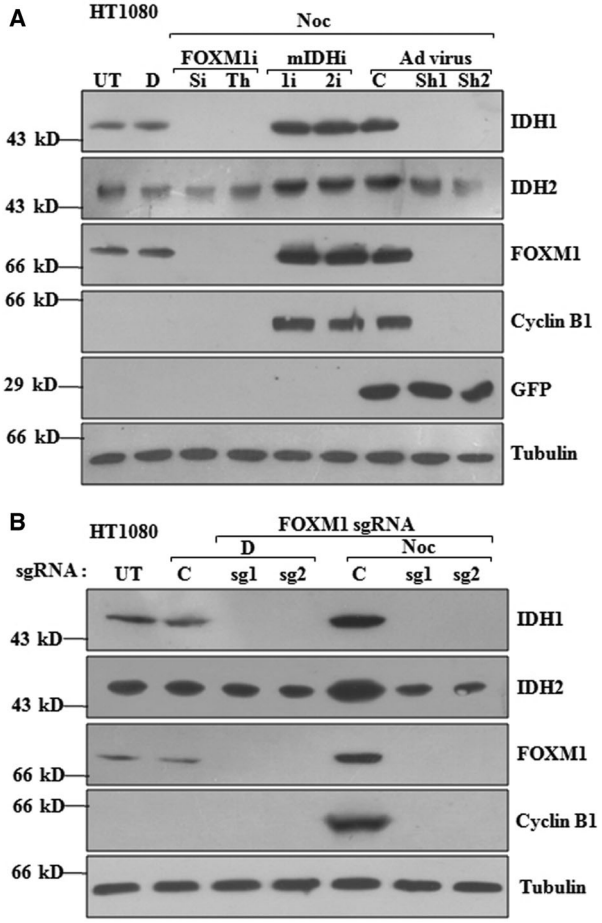


**Fig. 4.** Abrogation of FOXM1 depletes IDH1 protein. (A) HT1080 cells were treated with 3 μM of siomycin A, 10 μM of thiostreptron (FOXM1 inhibitors) or 10 μM of mutant IDH1i (AGI-5198) or mutant IDH2i (AGI-6870) or infected with control or FOXM1 shRNA viruses. Inhibitor and the viral infected dishes were co-treated with Noc for 18 h. UT, D (DMSO) and GFP served as controls. Equal amounts of protein were resolved and western blotting was performed. Blots are from experiments performed in duplicates, two times ($n$ = 4). (B) CRISPR/Cas9 was employed to deleted FOXM1 using two guide RNAs (sg1 and sg2) and a GFP sgRNA in HT1080 cells. Equal numbers of cells were plated in 60 mm dishes and were treated with Noc. WCLs were harvested and probed for indicated proteins and images representative of blots from three independent experiments ($n$ = 3).

in a promoterless-pGL4 vector and monitored the abundance of firefly luciferase protein under FOXM1 expression [20]. A dose-dependent increase in firefly luciferase protein levels was found in FOXM1 or ΔN-FOXM1 transfected cells (Fig. 5C). We generated two deletion constructs to delineate the putative FOXM1 binding region in the IDH1 promoter; these constructs harbour 532 bp and 219 bp of the promoter from transcription start site (TSS; Fig. S4A). Full-length clone of the IDH1 promoter was fully activated by FOXM1, but, luciferase protein levels remain unaltered in the 532 bp and 219 bp clone of IDH1 promoter (Fig. 5D). Therefore, we searched for any putative FOXM1 binding sites between −962 and −532 bp of IDH1 promoter. To activate expression of late genes, FOXM1 associates with the multi-molecular DREAM complex, LIN54 of the DREAM complex binds to the CHR sites in late gene promoters [54,55]. We found a CHR site in IDH1 promoter located at −818 bp from the TSS (Fig. S4B). SDM was performed to mutate the CHR site 'TTCGAG' to 'ATGCGG' in the full length IDH1 promoter. Co-transfection of the IDH1 promoter harbouring mutation in CHR site with FOXM1 did not activate firefly luciferase levels, similar to 532 and 219 bp of IDH1 promoter (Fig. 5E). To further confirm that, FOXM1 associates with IDH1 promoter we performed biotinylated DNA affinity purification assay. Here, biotinylated wild-type and mutant promoters of IDH1 were incubated with nuclear lysates of HEK 293T expressing Flag-FOXM1 and HA-LIN54 proteins (Fig. 5F–G). Immunoblot analysis show that FOXM1 and LIN54 associate with the wild-type IDH1 promoter, whereas genetic and pharmacological perturbation of FOXM1 disrupts FOXM1 binding to IDH1 promoter. Overall, FOXM1 activates IDH1 promoter and induces its protein levels.

## FOXM1 regulates D-2HG levels in G2/M

D-2HG is an oncometabolite produced in cells expressing mutants of IDH proteins; however, the production of D-2HG was never ascribed to any particular phase of the cell cycle. Since we found that IDH1 accumulates in G2/M, we assessed whether D-2HG levels increase as well (Figs 1 and 2). Initially, we validated our LC-MS/MS analysis in U87 and HT1080 which harbour wild-type and mutant IDH1, respectively. D-2HG levels were only detected in HT1080 and not in U87 cells expressing wild-type IDH proteins (Fig. 6A). Next, HT1080 cells were treated with various anti-mitotic agents for duration of 18 h; the cell lysates were processed and subjected to LC-MS/MS analysis. Anti-mitotic agents induced D-2HG levels to an average 4.5–5-fold compared to untreated, DMSO or doxorubicin controls (Fig. 6B). Furthermore, perturbation of FOXM1 down-regulates IDH1 protein; conversely, ectopic FOXM1 activates the latter (Figs 3, 4C–D and 3, 4A). Therefore, we assessed if D-2HG levels respond similarly to changes in FOXM1 protein levels. Noc or CA4-induced D-2HG levels decreased to baseline levels in FOXM1 shRNA infected cells; whereas levels of

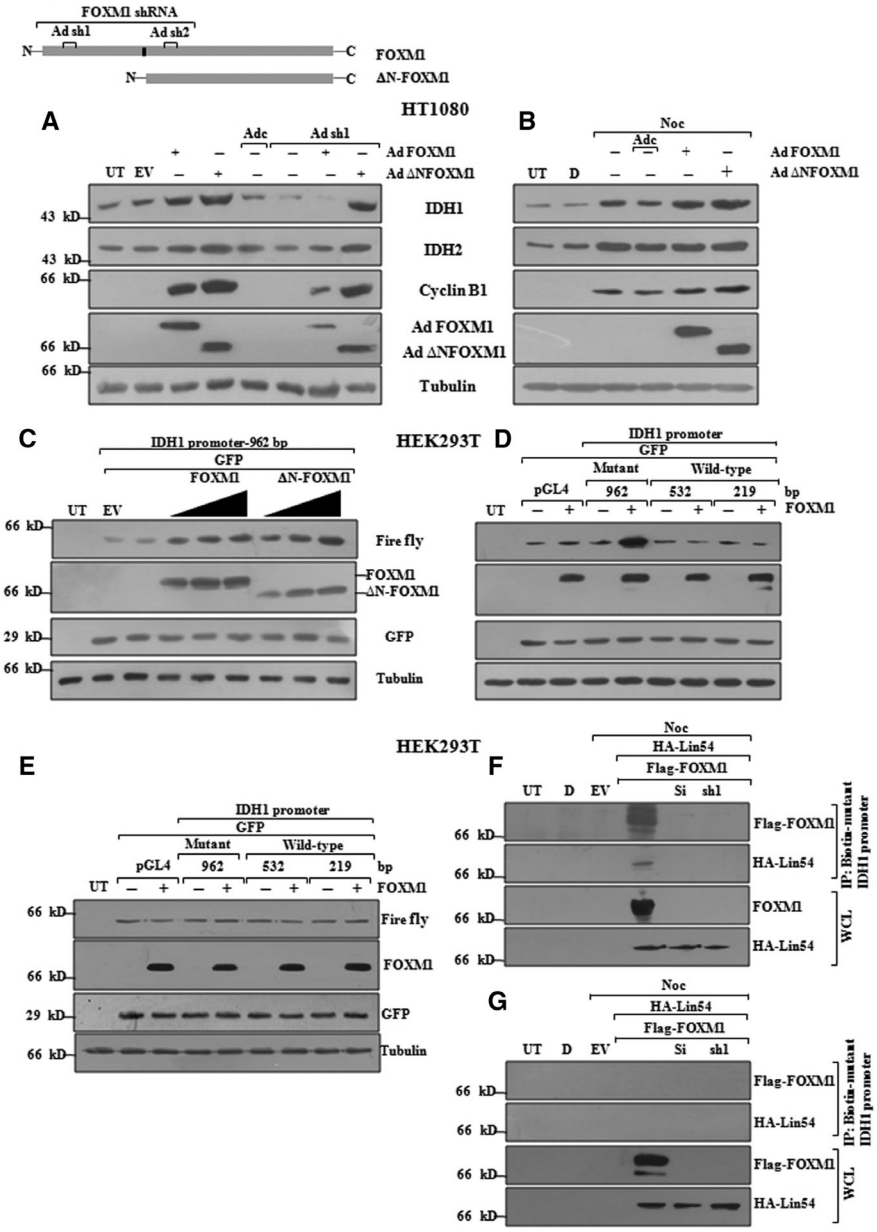


**Fig. 5.** FOXM1 activates IDH1 (A) HT1080 cells were infected with adenoviruses expressing T7 tagged full-length FOXM1 or ΔN-FOXM1 and co-infected with FOXM1 shRNA Adsh2 for 24 h as indicated. Adsh1 targets the N-terminal of FOXM1 and specifically reduces the full-length FOXM1 protein. Immunoblots were performed for IDH1, IDH2, Cyclin B1 and T7 tagged FOXM1 proteins. Blots are representative from two independent experiments done in duplicates ($n$ = 4). (B) HT1080 cells were infected with full-length FOXM1 or ΔN-FOXM1 and co-treated with Noc as shown. Images are from three independent experiments ($n$ = 3). (C) Five hundred nanogram of IDH1-promoter was co-transfected with increasing amounts of FOXM1 or ΔN-FOXM1 with GFP for 24 h. Expression plasmids were of 100, 250 and 500 ng concentrations. WCL were probed for firefly luciferase and T7-FOXM1. GFP was used as transfection control and tubulin as loading control. Blots shown are representative of three experiments performed in duplicates ($n$ = 6). (D) Five hundred nanogram of IDH1 promoter or deletion constructs of 532, and 219 bp were co-transfected with 500 ng of T7-FOXM1, 200 ng of GFP plasmids for 24 h. Plasmid concentration was made upto 2 μg by using salmon sperm DNA and transfected with PEI. Blots shown are representative of three experiments performed in duplicates ($n$ = 6). (E) FOXM1 binding site mutated in the full length IDH1- promoter of 962 bp was not responsive to ectopic FOXM1 protein. (F, G) Biotinylated DNA probes of human IDH1 promoter with or without FOXM1 binding site mutation was incubated with nuclear extracts of Noc treated HEK 293T cells co-transfected with Flag-FOXM1 and HA-Lin54. Here, Siomycin A and FOXM1 shRNA were used to downregulate FOXM1 protein and subjected to DNA affinity purification.

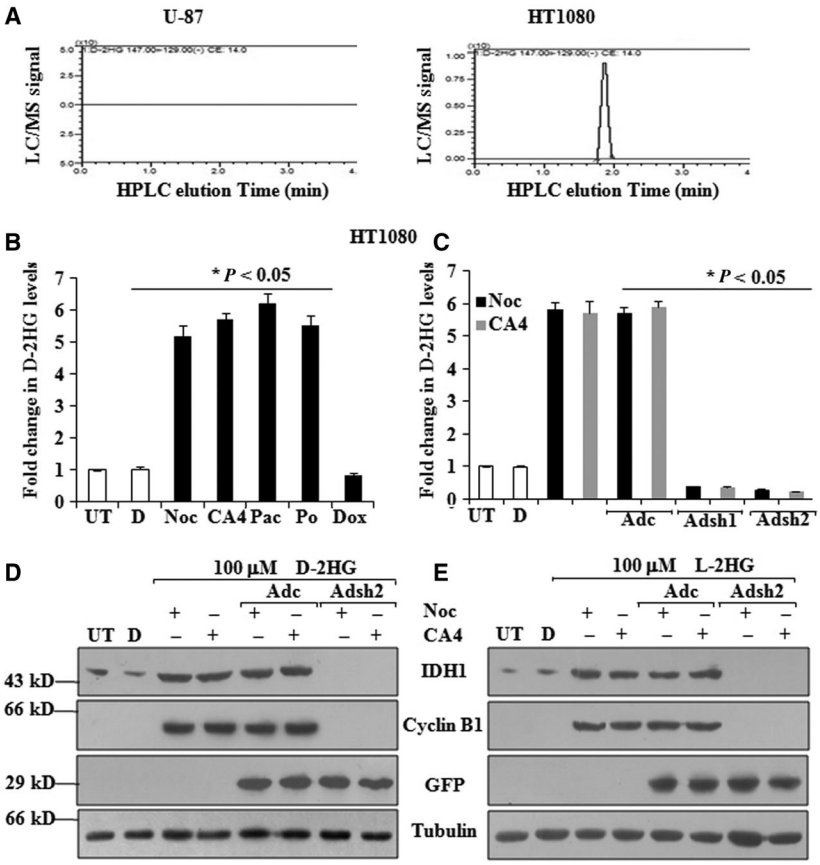


**Fig. 6.** Maximal D-2HG levels in G2/M arrested HT1080 cells are regulated by FOXM1. (A) D-2HG in U87$^{IDH1/IDH1}$ and HT1080$^{IDH1/IDH1\text{-}R132C}$ were analysed using LC-MS/MS. (B) HT1080 cells were treated with 500 nM of various mitotic blockers for 18 h. Metabolites were extracted by using 80 : 20 (methanol : water) at −80°C and dissolved in LC-MS/MS buffer and analysed for D-2HG. Fold change in D-2HG levels relative to control is shown. Experiments were performed independently two times in triplicates ($n$ = 6). (C) HT1080 cells were either infected with a control shRNA or FOXM1 shRNAs for 2 h and then treated with Noc or CA4 for 18 h. Similar to A, D-2HG levels were analysed and shown. Experiments were performed independently two times in triplicates ($n$ = 6). (D, E) HT1080 cells infected with control or FOXM1 shRNAs and later treated either with Noc or CA4 for 18 h as indicated. 100 µM of D-2HG or L-2HG was also added to Noc and CA4 treated cells. IDH1 and Cyclin B1 levels were determined with appropriate antibodies. Blots are representative from three independent experiments, ($n$ = 3).

D-2HG are unchanged in scrambled shRNA infected or untreated cells (Fig. 6C). D-2HG is known to trigger a change in the methylation landscape of mIDH1 protein expressing cells. Consequently, large-scale changes in gene expression are seemingly wrought by D-2HG [49,56]. Therefore, we checked whether IDH1 protein levels are modulated by D-2HG treatments, so HT1080 cells infected with FOXM1 shRNAs were co-treated with Noc or D-2HG/L-2HG or both. IDH1 protein levels were neither affected by D-2HG or L-2HG. However, ablated IDH1 protein levels in Noc-treated cells were exclusive to depletion of FOXM1 irrespective of D- or L-2HG treatments (Fig. 6D–E). In combination, these results suggest that D-2HG levels are maximum in Noc-arrested cells and knock-down of FOXM1 not only down-regulates IDH1 protein, but also its onco-metabolite D-2HG.

## Discussion

In this study, we demonstrate that expression of IDH1 and IDH2 are cell cycle regulated, where basal levels of the proteins peak to maximum in G2/M. Tubulin inhibitors, and not doxorubicin induce IDH1 and IDH2 proteins. Genetic or inhibitor-based ablation of FOXM1 blocks cell cycle or Noc-induced IDH1. In comparison, overexpression of either wild-type or hyperactive FOXM1 strongly activates IDH1 protein levels. Higher D-2HG levels correspond to more IDH1 protein in G2/M, and depletion of FOXM1 decreases D-2HG abundance.

Earlier reports did not assign the expression of IDH proteins to any particular phase of the cell cycle. Mutant-specific inhibitors of IDH proteins do not arrest cells in G2/M as compared to Cdk1or Plk1 inhibitors [57–60]. Moreover, mutant IDH1 inhibitors induce a small spurt in cell growth [61]. Therefore, blockade of IDH1 or IDH2 could not provide any insight into their cell cycle dependencies. However, results from our study indicate that IDH1 and IDH2 are maximally expressed in G2/M. Among them, first, in synchronized cells, IDH proteins levels peak similar to Cyclin B1, a master regulator of mitosis. In addition, IDH and Cyclin B1 proteins wane after 15 h; an inherent propensity of mitotic proteins to drop levels after cell division (Fig. 1A). Next, in anti-mitotic agent treated cells, maximal IDH protein levels corroborate with increased pH3Ser10 and Cyclin B1 (Fig 2A).

Third, FOXM1 transcriptionally regulates many mitotic genes, with Cyclin B1 as one of them [50]. As a result FOXM1 not only down-regulated Cyclin B1 but also IDH1 protein levels (Fig. 3). Next, D-2HG levels are the highest in G2/M (Fig. 6B). Overall, our findings show that G2/M harbours maximal levels of IDH1 and IDH2 proteins and D-2HG.

An IDH1 mutation is an early event in gliomas; it even precedes the co-deletion of 1p/19q [62]. Recently, IDH1 status was used as a molecular determinant to classify brain tumours [63]. But, how IDH1 protein levels are sustained in various grades of gliomas is elusive. It was shown that FOXM1 locus was amplified in 20% of IDH1 mutant-glioma patients and was linked to tumour progression. Further, a network of genes upregulated by FOXM1 was found in 85% of these patients [64]. In our study, FOXM1 robustly activates IDH1 promoter, transcript and protein, and perturbation of FOXM1 abrogates IDH1 protein levels. Thus, it is likely that aberrant FOXM1 protein found in IDH1-mutant gliomas may regulate IDH1. FOXM1 has been shown to associate with the multiprotein DREAM complex to precisely activate late gene expressions. The DREAM complex binds to CHR sites in late gene promoters and recruits FOXM1 to transactivate gene expression in G2/M [24,25,65]. To support this, we identified a CHR site in IDH1 promoter responsive to FOXM1 mediated-activation. Furthermore, Lin54, the protein that anchors DREAM complex to CHR site also binds to IDH1 promoter [54].

SREBP1a and SREBP2 were also found to transcriptionally regulate IDH1 in sterol-deficient conditions, therefore IDH1 is regulated by different transcription factors in cue to cellular pathways [19,20]. However, in HT1080 synchronized cells, IDH1 protein levels are maintained at basal levels from G1/S boundary to G2/M (Fig. 1A–C). We found that basal IDH1 protein levels are absent in FOXM1 knock-out HT1080 cell lines (Fig. 4B). Thus, FOXM1 governs basal and late expressions of IDH1 protein levels in chondrosarcoma cells. In contrast, FOXM1 marginally contributes to IDH2 regulation in G2/M. It is possible that FOXM1 cooperates with some other transcription factors to optimally activate IDH2 in G2/M. Active site IDH mutants equip the enzyme with a neomorphic activity, which leads to the overproduction of D-2HG from α-KG [49,56]. Consequently, in mIDH1 cells, D-2HG accumulates upto 35 mM as a dead-end metabolite [5]. Therefore, D-2HG was assumed to be constitutively produced by mIDH1 protein. Unlike D-2HG, the other enantiomer L-2HG was shown to be highly induced under hypoxia than in normoxic conditions. Blockade of either malate or lactate dehydrogenase enzymes in hypoxic cells efficiently reduced L-2HG levels [10,11]. Here, we show that in normoxia, D-2HG is maximally produced only during G2/M. Abrogation of FOXM1 protein by two different shRNAs decreases D-2HG levels. Notably, we found that D-2HG levels are 4.5-fold more in G2/M than in asynchronous cells (Fig 6B–C). Thus, in HT1080 it is likely that D-2HG levels too may fall after cell division similar to IDH1 protein (Fig 1A). Taken together, D-2HG levels may also be cell cycle regulated as IDH1. Further, low grade and secondary IDH1 mutant gliomas are variably associated with co-deletion of chromosome 1p/19q [63], thus it is likely that spurt of D-2HG levels in G2/M may contribute to chromosomal aberrations with disease progression.

Patients bearing mutant IDH1 gliomas exhibit better survival rates in response to chemotherapy, radiation and live longer [66–69]. Thus, to block mutant IDH1 activity, mutant-specific IDH1 inhibitors are in various stages of trials and may enter clinics as precision medicine [70]. However, in comparison to wild-type IDH1, mutant IDH1 expressing cells are endowed with higher sensitivity to radiation and chemotherapy as they exhibit higher levels of reactive oxygen species, and breaks in DNA causing cell death. In contrast, treatments with mIDH1i circumvent the sensitivity of mutant IDH1 cells to therapy leading to resistance [71–73]. Therefore, we suggest that FOXM1 maybe a better therapeutic target to abrogate mutant IDH1 expression in gliomas; as diverse chemical moieties inhibit FOXM1 in preclinical models leading to favourable outcomes [74,75].

## Acknowledgements

This work was supported by the Department of science and Technology (SB/YS/LS-42/2013), Department of Biotechnology (6242-P69/RGCB/PMD/DBT/NDJN/2015), India to NJ and senior research fellowship from University Grants Commission, India to KBBR. We thank Debanjan Bhattacharjee, Surbhi Lambhate and Hashnu Dutta for proof-reading the manuscript and Nagabhushana Ananthamurthy for critical review. We gratefully acknowledge DKIM of CSIR-IICT (IICT/pubs/2018/226).

## Author contributions

NJ conceived and managed the project. NJ and KBBR designed the experiments, analysed the data and wrote the manuscript. KBBR performed all the biological

experiments. Determination of D-2HG by LC/MS-MS was performed by KK, and analysed by VUMS.

## References


1 Mardis ER, Ding L, Dooling DJ, Larson DE, McLellan MD, Chen K, Koboldt DC, Fulton RS, Delehaunty KD, McGrath SD *et al.* (2009) Recurring mutations found by sequencing an acute myeloid leukemia genome. *N Engl J Med* **361**, 1058–1066.

2 Parsons DW, Jones S, Zhang X, Lin JC, Leary RJ, Angenendt P, Mankoo P, Carter H, Siu IM, Gallia GL *et al.* (2008) An integrated genomic analysis of human glioblastoma multiforme. *Science (New York, NY)* **321**, 1807–1812.

3 Amary MF, Damato S, Halai D, Eskandarpour M, Berisha F, Bonar F, McCarthy S, Fantin VR, Straley KS, Lobo S *et al.* (2011) Ollier disease and Maffucci syndrome are caused by somatic mosaic mutations of IDH1 and IDH2. *Nat Genet* **43**, 1262–1265.

4 Borger DR, Tanabe KK, Fan KC, Lopez HU, Fantin VR, Straley KS, Schenkein DP, Hezel AF, Ancukiewicz M, Liebman HM *et al.* (2012) Frequent mutation of isocitrate dehydrogenase (IDH)1 and IDH2 in cholangiocarcinoma identified through broad-based tumor genotyping. *Oncologist* **17**, 72–79.

5 Dang L, White DW, Gross S, Bennett BD, Bittinger MA, Driggers EM, Fantin VR, Jang HG, Jin S, Keenan MC *et al.* (2009) Cancer-associated IDH1 mutations produce 2-hydroxyglutarate. *Nature* **462**, 739–744.

6 Gelman SJ, Naser F, Mahieu NG, McKenzie LD, Dunn GP, Chheda MG and Patti GJ (2018) Consumption of NADPH for 2-HG synthesis increases pentose phosphate pathway flux and sensitizes cells to oxidative stress. *Cell Rep* **22**, 512–522.

7 Chowdhury R, Yeoh KK, Tian YM, Hillringhaus L, Bagg EA, Rose NR, Leung IK, Li XS, Woon EC, Yang M *et al.* (2011) The oncometabolite 2-hydroxyglutarate inhibits histone lysine demethylases. *EMBO Rep* **12**, 463–469.

8 Xu W, Yang H, Liu Y, Yang Y, Wang P, Kim SH, Ito S, Yang C, Wang P, Xiao MT *et al.* (2011) Oncometabolite 2-hydroxyglutarate is a competitive inhibitor of alpha-ketoglutarate-dependent dioxygenases. *Cancer Cell* **19**, 17–30.

9 Waitkus MS, Diplas BH and Yan H (2018) Biological role and therapeutic potential of IDH mutations in cancer. *Cancer Cell* **34**, 186–195.

10 Oldham WM, Clish CB, Yang Y and Loscalzo J (2015) Hypoxia-mediated increases in L-2-hydroxyglutarate coordinate the metabolic response to reductive stress. *Cell Metab* **22**, 291–303.

11 Intlekofer AM, Dematteo RG, Venneti S, Finley LW, Lu C, Judkins AR, Rustenburg AS, Grinaway PB, Chodera JD, Cross JR *et al.* (2015) Hypoxia induces production of L-2-hydroxyglutarate. *Cell Metab* **22**, 304–311.

12 Intlekofer AM, Wang B, Liu H and Shah H (2017) L-2-Hydroxyglutarate production arises from noncanonical enzyme function at acidic pH. *Nat Chem Biol* **13**, 494–500.

13 Tu BP, Kudlicki A, Rowicka M and McKnight SL (2005) Logic of the yeast metabolic cycle: temporal compartmentalization of cellular processes. *Science (New York, NY)* **310**, 1152–1158.

14 Almeida A, Bolanos JP and Moncada S (2010) E3 ubiquitin ligase APC/C-Cdh1 accounts for the Warburg effect by linking glycolysis to cell proliferation. *Proc Natl Acad Sci USA* **107**, 738–741.

15 Colombo SL, Palacios-Callender M, Frakich N, Carcamo S, Kovacs I, Tudzarova S and Moncada S (2011) Molecular basis for the differential use of glucose and glutamine in cell proliferation as revealed by synchronized HeLa cells. *Proc Natl Acad Sci USA* **108**, 21069–21074.

16 Jiang Y, Li X, Yang W, Hawke DH, Zheng Y, Xia Y, Aldape K, Wei C, Guo F, Chen Y *et al.* (2014) PKM2 regulates chromosome segregation and mitosis progression of tumor cells. *Mol Cell* **53**, 75–87.

17 Altman BJ, Hsieh AL, Sengupta A, Krishnanaiah SY, Stine ZE, Walton ZE, Gouw AM, Venkataraman A, Li B, Goraksha-Hicks P *et al.* (2015) MYC disrupts the circadian clock and metabolism in cancer cells. *Cell Metab* **22**, 1009–1019.

18 DeBose-Boyd RA and Ye J (2018) SREBPs in Lipid Metabolism, Insulin Signaling, and Beyond. *Trends Biochem Sci* **43**, 358–368.

19 Ricoult SJ, Dibble CC, Asara JM and Manning BD (2016) Sterol regulatory element binding protein regulates the expression and metabolic functions of wild-type and oncogenic IDH1. *Mol Cell Biol* **36**, 2384–2395.

20 Shechter I, Dai P, Huo L and Guan G (2003) IDH1 gene transcription is sterol regulated and activated by SREBP-1a and SREBP-2 in human hepatoma HepG2 cells: evidence that IDH1 may regulate lipogenesis in hepatic cells. *J Lipid Res* **44**, 2169–2180.

21 Tia N, Singh AK, Pandey P, Azad CS, Chaudhary P and Gambhir IS (2018) Role of Forkhead Box O (FOXO) transcription factor in aging and diseases. *Gene* **648**, 97–105.

22 Charitou P, Rodriguez-Colman M, Gerrits J, van Triest M, Groot Koerkamp M, Hornsveld M, Holstege F, Verhoeven-Duif NM and Burgering BM (2015) FOXOs support the metabolic requirements of normal and tumor cells by promoting IDH1 expression. *EMBO Rep* **16**, 456–466.

23 Yang X, Du T, Wang X, Zhang Y, Hu W, Du X, Miao L and Han C (2015) IDH1, a CHOP and C/EBPbeta-responsive gene under ER stress, sensitizes human

melanoma cells to hypoxia-induced apoptosis. *Cancer Lett* **365**, 201–210.
24 Sadasivam S and DeCaprio JA (2013) The DREAM complex: master coordinator of cell cycle-dependent gene expression. *Nat Rev Cancer* **13**, 585–595.
25 Sadasivam S, Duan S and DeCaprio JA (2012) The MuvB complex sequentially recruits B-Myb and FoxM1 to promote mitotic gene expression. *Genes Dev* **26**, 474–489.
26 Liao GB, Li XZ, Zeng S, Liu C, Yang SM, Yang L, Hu CJ and Bai JY (2018) Regulation of the master regulator FOXM1 in cancer. *Cell Commun Signal* **16**, 57.
27 Boussif O, Lezoualc'h F, Zanta MA, Mergny MD, Scherman D, Demeneix B and Behr JP (1995) A versatile vector for gene and oligonucleotide transfer into cells in culture and *in vivo*: polyethylenimine. *Proc Natl Acad Sci USA* **92**, 7297–7301.
28 Rajendra Y, Kiseljak D, Baldi L, Wurm FM and Hacker DL (2015) Transcriptional and post-transcriptional limitations of high-yielding, PEI-mediated transient transfection with CHO and HEK-293E cells. *Biotechnol Prog* **31**, 541–549.
29 Vangala JR, Dudem S, Jain N and Kalivendi SV (2014) Regulation of PSMB5 protein and beta subunits of mammalian proteasome by constitutively activated signal transducer and activator of transcription 3 (STAT3): potential role in bortezomib-mediated anticancer therapy. *The Journal of biological chemistry*. **289**, 12612–12622.
30 Jain N, Gupta S, Sudhakar C, Radha V and Swarup G (2005) Role of p73 in regulating human caspase-1 gene transcription induced by interferon-{gamma} and cisplatin. *J Biol Chemi* **280**, 36664–36673.
31 Zheng L, Baumann U and Reymond JL (2004) An efficient one-step site-directed and site-saturation mutagenesis protocol. *Nucleic Acids Res* **32**, e115.
32 Haan C and Behrmann I (2007) A cost effective non-commercial ECL-solution for Western blot detections yielding strong signals and low background. *J Immunol Methods* **318**, 11–19.
33 Park HJ, Wang Z, Costa RH, Tyner A, Lau LF and Raychaudhuri P (2008) An N-terminal inhibitory domain modulates activity of FoxM1 during cell cycle. *Oncogene* **27**, 1696–1704.
34 Sanjana NE, Shalem O and Zhang F (2014) Improved vectors and genome-wide libraries for CRISPR screening. *Nat Methods* **11**, 783–784.
35 Shalem O, Sanjana NE, Hartenian E, Shi X, Scott DA, Mikkelson T, Heckl D, Ebert BL, Root DE, Doench JG *et al.* (2014) Genome-scale CRISPR-Cas9 knockout screening in human cells. *Science (New York, NY)* **343**, 84–87.
36 Chen H, Yang C, Yu L, Xie L, Hu J, Zeng L and Tan Y (2012) Adenovirus-mediated RNA interference targeting FOXM1 transcription factor suppresses cell proliferation and tumor growth of nasopharyngeal carcinoma. *J Gene Med* **14**, 231–240.
37 Yang C, Chen H, Yu L, Shan L, Xie L, Hu J, Chen T and Tan Y (2013) Inhibition of FOXM1 transcription factor suppresses cell proliferation and tumor growth of breast cancer. *Cancer Gene Ther* **20**, 117–124.
38 Jain N, Sudhakar C and Swarup G (2007) Tumor necrosis factor-alpha-induced caspase-1 gene expression. Role of p73. *FEBS J* **274**, 4396–407.
39 He TC, Zhou S, da Costa LT, Yu J, Kinzler KW and Vogelstein B (1998) A simplified system for generating recombinant adenoviruses. *Proc Natl Acad Sci USA* **95**, 2509–2514.
40 Kumar K, Siva B, Sarma VUM, Mohabe S, Reddy AM, Boustie J, Tiwari AK, Rao NR and Babu KS (2018) UPLC-MS/MS quantitative analysis and structural fragmentation study of five Parmotrema lichens from the Eastern Ghats. *J Pharm Biomed Anal* **156**, 45–57.
41 Muller GA, Quaas M, Schumann M, Krause E, Padi M, Fischer M, Litovchick L, DeCaprio JA and Engeland K (2012) The CHR promoter element controls cell cycle-dependent gene transcription and binds the DREAM and MMB complexes. *Nucleic Acids Res* **40**, 1561–1578.
42 Muller GA, Wintsche A, Stangner K, Prohaska SJ, Stadler PF and Engeland K (2014) The CHR site: definition and genome-wide identification of a cell cycle transcriptional element. *Nucleic Acids Res* **42**, 10331–10350.
43 Bansal M, Moharir SC, Sailasree SP, Sirohi K, Sudhakar C, Sarathi DP, Lakshmi BJ, Buono M, Kumar S and Swarup G (2018) Optineurin promotes autophagosome formation by recruiting the autophagy-related Atg12-5-16L1 complex to phagophores containing the Wipi2 protein. *J Biol Chem* **293**, 132–147.
44 Tonjes M, Barbus S, Park YJ, Wang W, Schlotter M, Lindroth AM, Pleier SV, Bai AHC, Karra D, Piro RM *et al.* (2013) BCAT1 promotes cell proliferation through amino acid catabolism in gliomas carrying wild-type IDH1. *Nat Med* **19**, 901–908.
45 Grassian AR, Parker SJ, Davidson SM, Divakaruni AS, Green CR, Zhang X, Slocum KL, Pu M, Lin F, Vickers C *et al.* (2014) IDH1 mutations alter citric acid cycle metabolism and increase dependence on oxidative mitochondrial metabolism. *Can Res* **74**, 3317–3331.
46 Sawicka A and Seiser C (2012) Histone H3 phosphorylation - a versatile chromatin modification for different occasions. *Biochimie* **94**, 2193–2201.
47 Zeng L, Morinibu A, Kobayashi M, Zhu Y, Wang X, Goto Y, Yeom CJ, Zhao T, Hirota K, Shinomiya K *et al.* (2015) Aberrant IDH3alpha expression promotes malignant tumor growth by inducing HIF-1-mediated metabolic reprogramming and angiogenesis. *Oncogene* **34**, 4758–4766.

48 Tron GC, Pirali T, Sorba G, Pagliai F, Busacca S and Genazzani AA (2006) Medicinal chemistry of combretastatin A4: present and future directions. *J Med Chem* **49**, 3033–3044.
49 Ye D, Guan KL and Xiong Y (2018) Metabolism, activity, and targeting of D- and L-2-hydroxyglutarates. *Trends Cancer* **4**, 151–165.
50 Leung TW, Lin SS, Tsang AC, Tong CS, Ching JC, Leung WY, Gimlich R, Wong GG and Yao KM (2001) Over-expression of FoxM1 stimulates cyclin B1 expression. *FEBS Lett* **507**, 59–66.
51 Bhat UG, Halasi M and Gartel AL (2009) Thiazole antibiotics target FoxM1 and induce apoptosis in human cancer cells. *PLoS ONE* **4**, e5592.
52 Rohle D, Popovici-Muller J, Palaskas N, Turcan S, Grommes C, Campos C, Tsoi J, Clark O, Oldrini B, Komisopoulou E *et al.* (2013) An inhibitor of mutant IDH1 delays growth and promotes differentiation of glioma cells. *Science (New York, NY)* **340**, 626–630.
53 Wang F, Travins J, DeLaBarre B, Penard-Lacronique V, Schalm S, Hansen E, Straley K, Kernytsky A, Liu W, Gliser C *et al.* (2013) Targeted inhibition of mutant IDH2 in leukemia cells induces cellular differentiation. *Science (New York, NY)* **340**, 622–626.
54 Schmit F, Cremer S and Gaubatz S (2009) LIN54 is an essential core subunit of the DREAM/LINC complex that binds to the cdc2 promoter in a sequence-specific manner. *FEBS J* **276**, 5703–5716.
55 Fischer M and Muller GA (2017) Cell cycle transcription control: DREAM/MuvB and RB-E2F complexes. *Crit Rev Biochem Mol Biol* **52**, 638–662.
56 M Gagné L, Boulay K, Topisirovic I, Huot MÉ and Mallette FA (2017) Oncogenic activities of IDH1/2 mutations: from epigenetics to cellular signaling. *Trends Cell Biol* **27**, 738–752.
57 Vassilev LT, Tovar C, Chen S, Knezevic D, Zhao X, Sun H, Heimbrook DC and Chen L (2006) Selective small-molecule inhibitor reveals critical mitotic functions of human CDK1. *Proc Natl Acad Sci USA* **103**, 10660–10665.
58 Li L, Paz AC, Wilky BA, Johnson B, Galoian K, Rosenberg A, Hu G, Tinoco G, Bodamer O and Trent JC (2015) Treatment with a small molecule mutant IDH1 inhibitor suppresses tumorigenic activity and decreases production of the oncometabolite 2-hydroxyglutarate in human chondrosarcoma cells. *PLoS ONE* **10**, e0133813.
59 Yen K, Travins J, Wang F, David MD, Artin E, Straley K, Padyana A, Gross S, DeLaBarre B, Tobin E *et al.* (2017) AG-221, a first-in-class therapy targeting acute myeloid leukemia harboring oncogenic IDH2 mutations. *Cancer Discov* **7**, 478–493.
60 Steegmaier M, Hoffmann M, Baum A, Lenart P, Petronczki M, Krssak M, Gurtler U, Garin-Chesa P, Lieb S, Quant J *et al.* (2007) BI 2536, a potent and selective inhibitor of polo-like kinase 1, inhibits tumor growth *in vivo*. *Curr Biol* **17**, 316–322.
61 Tateishi K, Wakimoto H, Iafrate AJ, Tanaka S, Loebel F, Lelic N, Wiederschain D, Bedel O, Deng G, Zhang B *et al.* (2015) Extreme Vulnerability of IDH1 mutant cancers to NAD+ depletion. *Cancer Cell* **28**, 773–784.
62 Watanabe T, Nobusawa S, Kleihues P and Ohgaki H (2009) IDH1 mutations are early events in the development of astrocytomas and oligodendrogliomas. *Am J Pathol* **174**, 1149–1153.
63 Louis DN, Perry A, Reifenberger G, von Deimling A, Figarella-Branger D, Cavenee WK, Ohgaki H, Wiestler OD, Kleihues P and Ellison DW (2016) The 2016 World Health Organization Classification of tumors of the central nervous system: a summary. *Acta Neuropathol* **131**, 803–820.
64 Bai H, Harmancı AS, Erson-Omay EZ, Li J, Coşkun S, Simon M, Krischek B, Özduman K, Omay SB, Sorensen EA *et al.* (2015) Integrated genomic characterization of IDH1-mutant glioma malignant progression. *Nat Genet* **48**, 59.
65 Grant GD, Brooks L 3rd, Zhang X, Mahoney JM, Martyanov V, Wood TA, Sherlock G, Cheng C and Whitfield ML (2013) Identification of cell cycle-regulated genes periodically expressed in U2OS cells and their regulation by FOXM1 and E2F transcription factors. *Mol Biol Cell* **24**, 3634–3650.
66 Bleeker FE, Atai NA, Lamba S, Jonker A, Rijkeboer D, Bosch KS, Tigchelaar W, Troost D, Vandertop WP, Bardelli A *et al.* (2010) The prognostic IDH1( R132) mutation is associated with reduced NADP+-dependent IDH activity in glioblastoma. *Acta Neuropathol* **119**, 487–494.
67 Yan H, Parsons DW, Jin G, McLendon R, Rasheed BA, Yuan W, Kos I, Batinic-Haberle I, Jones S, Riggins GJ *et al.* (2009) IDH1 and IDH2 mutations in gliomas. *N Engl J Med* **360**, 765–773.
68 Mohrenz IV, Antonietti P, Pusch S, Capper D, Balss J, Voigt S, Weissert S, Mukrowsky A, Frank J, Senft C *et al.* (2013) Isocitrate dehydrogenase 1 mutant R132H sensitizes glioma cells to BCNU-induced oxidative stress and cell death. *Apoptosis* **18**, 1416–1425.
69 Li S, Chou AP, Chen W, Chen R, Deng Y, Phillips HS, Selfridge J, Zurayk M, Lou JJ, Everson RG *et al.* (2013) Overexpression of isocitrate dehydrogenase mutant proteins renders glioma cells more sensitive to radiation. *Neuro Oncol* **15**, 57–68.
70 Dang L and Su SM (2017) Isocitrate dehydrogenase mutation and (R)-2-hydroxyglutarate: from basic discovery to therapeutics development. *Annu Rev Biochem* **86**, 305–331.
71 Molenaar RJ, Botman D, Smits MA, Hira VV, van Lith SA, Stap J, Henneman P, Khurshed M, Lenting

K, Mul AN *et al*. (2015) Radioprotection of IDH1-mutated cancer cells by the IDH1-mutant inhibitor AGI-5198. *Can Res* **75**, 4790–4802.

72 Lu Y, Kwintkiewicz J, Liu Y, Tech K, Frady LN, Su YT, Bautista W, Moon SI, MacDonald J, Ewend MG *et al*. (2017) Chemosensitivity of IDH1-mutated gliomas due to an impairment in PARP1-mediated DNA repair. *Can Res* **77**, 1709–1718.

73 Khurshed M, Aarnoudse N, Hulsbos R, Hira VVV, van Laarhoven HWM, Wilmink JW, Molenaar RJ and van Noorden CJF (2018) IDH1-mutant cancer cells are sensitive to cisplatin and an IDH1-mutant inhibitor counteracts this sensitivity. *FASEB J* **32**, 6344–6352.

74 Gormally MV, Dexheimer TS, Marsico G, Sanders DA, Lowe C, Matak-Vinkovic D, Michael S, Jadhav A, Rai G, Maloney DJ *et al*. (2014) Suppression of the FOXM1 transcriptional programme via novel small molecule inhibition. *Nat Commun* **5**, 5165.

75 Hegde NS, Sanders DA, Rodriguez R and Balasubramanian S (2011) The transcription factor FOXM1 is a cellular target of the natural product thiostrepton. *Nat Chem* **3**, 725–731.

## Supporting information

Additional supporting information may be found online in the Supporting Information section at the end of the article.

**Fig. S1**. Synchronized cells harbour higher levels of IDH proteins in G2/M. HT1080 cells were synchronized using double-thymidine block and immunoblot analysis show that IDH1 and IDH2 proteins are expressed in a stage specific manner. Here IDH1 protein levels were detected using an antibody that binds a different epitope (336–350 amino acids). Cyclin B1 and pH3Ser10 proteins were used as positive controls for G2/M. Cyclin A was used as an S-phase marker and tubulin was used as a loading control. Blots shown are from two independent experiments ($n = 2$).

**Fig. S2**. Knock-down of FOXM1 in G2/M arrested cells down-regulates IDH1. Adenoviral FOXM1 shRNAs where infected for 2 h in A549, HeLa, MDA-MB-231 or MIA PaCa-2 cell lines. C, represents scrambled shRNA infection as control. Noc was added to uninfected and infected cells for 18 h. Immunoblotting for IDH1, IDH2, FOXM1 and Cyclin B1 proteins were performed. GFP was used as infection control and tubulin as the loading control. Blots shown are from two independent experiments performed in duplicates ($n = 4$).

**Fig. S3**. Overexpression of hyperactive FOXM1 induces IDH1 protein. A549, HeLa, MDA- MB-231 and MIA PaCa-2 cell lines were infected with DN-FOXM1 or control virus, C for 2 h. Cells were harvested after 24 h and WCL were subjected to immunoblotting for IDH1, IDH2, Cyclin B1 and Flag DN-FOXM1. GFP and tubulin were the infection and loading control. Blots shown are from two independent experiments performed in duplicates ($n = 4$).

**Fig. S4**. Human IDH1 promoter harbours cell cycle homology region. (A) Nucleotide sequence of IDH1 promoter showing previously characterized SREBP1a and SREB2, GC-Box element and CAAT box (10). CHR region is located upstream at −818 bp in IDH1 promoter. (B) Schematic representation of full length, 532 bp and 219 bp of IDH1 promoter.